Preprint, Institute of Mathematics, AS CR, Prague. 2008-1-1

Discrete maximum principle for 3D-FE solutions of the diffusion-reaction problem on prismatic meshes

Antti Hannukainen[1,*], Sergey Korotov[1,†], Tomáš Vejchodský[2,‡]

December 21, 2007

[1] Institute of Mathematics, Helsinki University of Technology
P.O. Box 1100, FIN–02015 Espoo, Finland
e-mail: antti.hannukainen, sergey.korotov@hut.fi

[2] Institute of Mathematics, Czech Academy of Sciences
Žitná 25, CZ–115 67 Prague 1, Czech Republic
e-mail: vejchod@math.cas.cz

Abstract: In this paper we analyse the discrete maximum principle (DMP) for a stationary diffusion-reaction problem solved by means of prismatic finite elements. We derive geometric conditions on the shape parameters of the prismatic partitions which guarantee validity of the DMP. The presented numerical tests show the sharpness of the obtained conditions.

Keywords: diffusion-reaction problem, maximum principle, prismatic finite elements, discrete maximum principle

Mathematics Subject Classification: 65N30, 65N50

1 Introduction

Mathematical models consisting of elliptic and parabolic partial differential equations with various boundary and initial conditions are useful tools in modeling and numerical simulations of various real-life problems (see, e.g., [7, 11]). Usually, the exact (classical) solutions of these models exhibits certain qualitative properties such as the maximum-minimum principle (or, as a particular case, the nonnegativity preservation) [24], the sign-stability (often called as a preservation of number of peaks) [14, 15], the maximum norm contractivity, etc. For more details in the subject see recent reviews [10, 18].

* The first author was supported by Project no. 211512 from the Academy of Finland.

† The second author was supported by the Academy Research Fellowship no. 208628 and Grant no. 121283 from the Academy of Finland.

‡ The third author was supported by Grant no. IAA100760702 of the Grant Agency of the Czech Academy of Sciences and by the institutional research plan no. AV0Z10190503 of the Czech Academy of Sciences.

Among these, the maximum principle is the basic characteristic usually associated with the second order elliptic (and parabolic) boundary value problems [17, 24, 26]. It can be mathematically described as an *a priori estimate* of the magnitude of the (unknown in the whole domain) solution by the magnitude of the (known) given, or easily computable, data. The maximum principle is not only a mathematical feature of the model but it also adequately describes the real behavior of the physical systems.

It is quite natural to require a suitable imitation of this property from the computed approximations. This is the reason why the construction and validity of the corresponding discrete analogues (the so-called discrete maximum principles, or DMPs in short) have drawn much attention. To the authors' knowledge, papers [28] by R. Varga in 1966 and [13] by H. Fujii in 1973 were probably the very first works aimed at construction of a reasonable DMP for elliptic and parabolic problems, respectively. These original papers as well as the presented work use special properties of the finite difference and finite element matrices to analyse the DMPs.

Later on, other types of the DMPs were formulated and proved in a number of papers, see, e.g., [6, 8, 17, 18, 21, 26, 29, 31]. They discuss various numerical methods for different problems and study the validity of the DMPs. Most attention was paid to the finite difference and finite element approximations of elliptic and parabolic problems and to various geometric conditions on the shape of the classical simplicial and block finite element partitions that provide the DMPs. Particularly challenging is the analysis of the DMPs for the less standard but more promising and economical higher order finite elements, see recent results [22] and [29]. However, the validity of the DMPs on prismatic meshes has not been considered so far in spite of the fact that the prismatic partitions can often be more natural and convenient compared to the standard tetrahedral partitions, especially for cylindrical 3D domains.

The paper is organized as follows. Section 2 describes the 3D diffusion-reaction model problem and Section 3 presents its finite element discretization by the lowest order prismatic elements. The main theoretical result about the DMP is contained in Section 4. Section 5 provides practical geometric conditions for prismatic partitions to guarantee the validity of the DMP. The sharpness of the obtained geometric conditions is verified by numerical tests in Section 6. Finally, Section 7 points out possible generalizations and several open problems.

2 Model problem

Throughout the paper we shall use the standard Sobolev space notation (cf. [7, 11]). We consider the following reaction-diffusion boundary value problem

$$-\Delta u + c\,u = f \quad \text{in } \Omega, \quad u = 0 \quad \text{on } \partial\Omega, \tag{1}$$

where $\Omega \subset \mathbf{R}^3$ is a bounded domain and c is a nonnegative bounded reaction coefficient. To define the weak solution of (1), we assume the boundary $\partial\Omega$ to be Lipschitz continuous, $f \in L^2(\Omega)$, $c \in L^\infty(\Omega)$, and

$$0 \le c \le \|c\|_{\infty,\Omega} < \infty, \tag{2}$$

where $\|c\|_{\infty,\Omega} = \|c\|_{L^\infty(\Omega)}$ stands for the L^∞-norm of the reaction coefficient c over the entire domain Ω. Similarly, we will use $\|c\|_{\infty,P}$ for the L^∞-norm of c over a subdomain $P \subset \Omega$.

The weak formulation of problem (1) reads: Find a function $u \in H_0^1(\Omega)$ such that

$$\int\limits_\Omega \nabla u \cdot \nabla v \,\mathrm{d}x + \int\limits_\Omega c\, uv \,\mathrm{d}x = \int\limits_\Omega f v \,\mathrm{d}x \qquad \forall v \in H_0^1(\Omega). \tag{3}$$

Under the above conditions the weak solution u exists and is unique.

The following theorem shows the continuous maximum principle (CMP) for problem (1), see [24] and also [17, 18] for a more general case of nonlinear problems with mixed boundary conditions. In the sequel the equalities and inequalities between functions from Lebesgue spaces should be understood up to a set of zero measure, as usually.

Theorem 1 *Let u be a solution to* (1) *corresponding to a right-hand side f. If $f \le 0$ and $u \in C(\overline{\Omega})$ then* $\max\limits_{\overline{\Omega}} u = 0$.

A natural discrete analogue to the above implication is known as the discrete maximum principle (DMP). In what follows, we formulate the DMP precisely and we derive geometric conditions on the shape of prismatic finite elements guaranteeing its validity.

3 FE discretization on prismatic meshes

Let $\Omega = \mathcal{G} \times \mathcal{I}$ be a cylindrical domain, where $\mathcal{G} \subset \mathbf{R}^2$ is a polygon, $\mathcal{I} = (0, z_0)$, and z_0 is a real positive number. We shall consider a face-to-face partition $\mathcal{T}_{h,\tau} = \mathcal{T}_h^{\mathcal{G}} \times \mathcal{T}_\tau^{\mathcal{I}}$ of $\overline{\Omega}$ into prisms (and call it *prismatic mesh* or *prismatic partition* of Ω), where $\mathcal{T}_h^{\mathcal{G}}$ is a triangulation of $\mathcal{G}$ and $\mathcal{T}_\tau^{\mathcal{I}}$ is a partition of $\mathcal{I}$ into segments (not necessarily with the same lengths). The prismatic elements of $\mathcal{T}_{h,\tau}$ will be denoted from now on with the symbol P possibly with certain subindices. The elements of the triangulation $\mathcal{T}_h^{\mathcal{G}}$ (being, actually, the bases of the prismatic elements) will be denoted by T possibly with subindices. Let $B_i,\ i = 1, \ldots, N + N^\partial$, be the vertices of $\mathcal{T}_{h,\tau}$, where $B_1, \ldots, B_N$ are the interior nodes and $B_{N+1}, \ldots, B_{N+N^\partial}$ belong to the boundary $\partial\Omega$.

Let $V_{h,\tau} \subset H_0^1(\Omega)$ be the finite element space associated to $\mathcal{T}_{h,\tau}$ and defined as follows:

$$\begin{aligned} V_{h,\tau} = \{\, \varphi \in H_0^1(\Omega) :\ & \varphi(x,y,z)|_P = \lambda(x,y) \cdot \ell(z),\ \text{where} \\ & \lambda(x,y) \in \mathbb{P}^1(T),\ \ell(z) \in \mathbb{P}^1(I),\ P = T \times I,\ P \in \mathcal{T}_{h,\tau},\ T \in \mathcal{T}_h^{\mathcal{G}},\ I \in T_\tau^{\mathcal{I}} \,\}, \end{aligned} \tag{4}$$

where $\mathbb{P}^1(T)$ and $\mathbb{P}^1(I)$ stand for the spaces of linear functions defined in the triangle T and in the interval I, respectively. Further, let $\phi_1, \ldots, \phi_N$ denote the standard finite element basis functions of $V_{h,\tau}$ satisfying $\phi_i(B_j) = \delta_{ij}$, $i = 1, 2, \ldots, N$, $j = 1, 2, \ldots, N + N^\partial$, where δ_{ij} is the Kronecker symbol.

The finite element discretization based on the weak formulation (3) reads: Find a function $u_{h,\tau} \in V_{h,\tau}$ such that

$$\int\limits_\Omega \nabla u_{h,\tau} \cdot \nabla v_{h,\tau} \,\mathrm{d}x + \int\limits_\Omega c\, u_{h,\tau} v_{h,\tau} \,\mathrm{d}x = \int\limits_\Omega f v_{h,\tau} \,\mathrm{d}x \qquad \forall v_{h,\tau} \in V_{h,\tau}. \tag{5}$$

4 Discrete maximum principle

The discrete problem introduced above should, ideally, satisfy the following natural property (cf. [8, 17, 18, 21, 29]):

$$f \leq 0 \quad \Longrightarrow \quad \max_{\overline{\Omega}} u_{h,\tau} = 0. \tag{6}$$

This implication, however, has two different interpretations which are precisely formulated in the following definitions.

Definition 1 *Let $\mathcal{T}_{h,\tau}$ be a partition of Ω and let $V_{h,\tau}$ given by (4) be the finite element space based on $\mathcal{T}_{h,\tau}$. We say that approximate problem (5) satisfies the discrete maximum principle (DMP) if*

$$\max_{\overline{\Omega}} u_{h,\tau} = 0 \quad \textit{for all} \quad f \leq 0. \tag{7}$$

Definition 2 *Let $f \leq 0$ be the right-hand side and let $\mathcal{T}_{h,\tau}$ be a partition of Ω. We say that approximate problem (5) satisfies the discrete maximum principle (DMP) if*

$$\max_{\overline{\Omega}} u_{h,\tau} = 0. \tag{8}$$

If we consider a partition $\mathcal{T}^A_{h,\tau}$ such that problem (5) satisfies the DMP according to Definition 1, implication (6) is valid for all nonpositive right-hand sides f. On the other hand, if a right-hand side $f_1^B \leq 0$ and a partition $\mathcal{T}^B_{h,\tau}$ are such that the DMP by Definition 2 is valid then there could exist another right-hand side $f_2^B \leq 0$ such that the corresponding approximate solution $u_{h,\tau}$ obtained on the same mesh $\mathcal{T}^B_{h,\tau}$ does not satisfy (6).

To prove the DMP according to Definition 1 we have to characterize a suitable class of meshes that guarantee (7). On the other hand, to prove the DMP according to Definition 2 we take an arbitrary nonpositive right-hand side f and construct a suitable mesh according to this particular f such that (8) is valid.

In what follows we consider the DMP according to Definition 1. Theorem 2 below gives sufficient conditions for prismatic partitions guaranteeing (7).

Remark 1 As all the basis functions are nonnegative, it is obvious that the FE approximation satisfies $u_{h,\tau} \leq 0$ everywhere in Ω if and only if $u_{h,\tau}$ has nonpositive values at all nodal points $B_i,\ i = 1, \ldots, N + N^\partial$.

Letting $u_{h,\tau} = \sum_{i=1}^{N} y_i \phi_i$, we come to the system of N linear equations

$$\mathbf{A}\mathbf{y} = \mathbf{F}, \tag{9}$$

where $\mathbf{A} = (a_{ij})_{i,j=1}^N$ is called the *FE matrix*, the vector of unknowns $\mathbf{y} = (y_1, \ldots, y_N)^\top$ consists of the values of $u_{h,\tau}$ at the interior nodes, and the vector $\mathbf{F} = (F_1, \ldots, F_N)^\top$ is known as the *load vector*. The entries of the matrix $\mathbf{A}$ and of the vector $\mathbf{F}$ associated to problem (1) are

$$a_{ij} = \int_\Omega \nabla\phi_i \cdot \nabla\phi_j \,\mathrm{d}x + \int_\Omega c\,\phi_i\phi_j \,\mathrm{d}x = a_{ij}^{(1)} + a_{ij}^{(2)}, \tag{10}$$

$$F_i = \int\limits_\Omega f \phi_i \, \mathrm{d}x, \tag{11}$$

where matrices $\mathbf{A}^{(1)} = (a_{ij}^{(1)})_{i,j=1}^N$ and $\mathbf{A}^{(2)} = (a_{ij}^{(2)})_{i,j=1}^N$ are referred to as the *stiffness* and *mass matrices*, respectively.

Various geometric conditions on the shape of the simplices in FE partitions come, in fact, from the set of algebraic requirements on the entries of $\mathbf{A}$ providing the validity of the DMPs, as it is done for example in [6, 17, 21]), where $\mathbf{A}$ is assumed to be irreducibly diagonally dominant.

However, we find that it is sufficient and more convenient to require the matrix $\mathbf{A}$ to be a Stieltjes matrix, i.e., symmetric, positive definite and having nonpositive off-diagonal entries. Notice that Stieltjes matrices form a subclass of M-matrices which are not required to be symmetric [27, p. 85] or [12, p. 121]. M-matrices have nonpositive inverse, which is a sufficient and necessary condition for the DMP in the sense of Definition 1 and a sufficient condition for the DMP in the sense of Definition 2. In the case of Stieltjes matrices we avoid checking the irreducibility of the finite element matrix which is not always true (cf. [9, p. 4]) and, moreover, it might be difficult to verify, in general.

Before we formulate the main result, we prove three auxiliary lemmas, where we compute the entries of the local stiffness and mass matrices for an interval, a triangle, and a prism. In the sequel, the symbol $|T|$ stands for the measure of the set T.

Lemma 1 *Let $I = (0, d)$ be an interval and let $\ell_0(z) = 1 - z/d$ and $\ell_1(z) = z/d$ be the 1D shape functions, see Figure 1. Then*

$$\int_I \ell_0^2 \, \mathrm{d}z = \int_I \ell_1^2 \, \mathrm{d}z = d/3, \qquad \int_I \ell_0 \ell_1 \, \mathrm{d}z = d/6, \tag{12}$$

$$\int_I (\ell_0')^2 \, \mathrm{d}z = \int_I (\ell_1')^2 \, \mathrm{d}z = 1/d, \qquad \int_I \ell_0' \ell_1' \, \mathrm{d}z = -1/d. \tag{13}$$

P r o o f : It follows from a straightforward calculation. ■

Lemma 2 *Let T be a triangle ABC with the corresponding angles α, β, and γ, see Figure 1. Let $\lambda_A = \lambda_A(x, y)$ and $\lambda_B = \lambda_B(x, y)$ be the barycentric coordinates or equivalently the linear shape functions corresponding to the vertices A and B. Then*

$$\int_T \lambda_A^2 \, \mathrm{d}(x, y) = |T|/6, \tag{14}$$

$$\int_T \lambda_A \lambda_B \, \mathrm{d}(x, y) = |T|/12, \tag{15}$$

$$\int_T |\nabla \lambda_A|^2 \, \mathrm{d}(x, y) = \frac{1}{2}(\cot \beta + \cot \gamma), \tag{16}$$

$$\int_T \nabla \lambda_A \cdot \nabla \lambda_B \, \mathrm{d}(x, y) = -\frac{1}{2} \cot \gamma. \tag{17}$$

P r o o f : Results (14) and (15) follow immediately from a general formula

$$\int_T \lambda_A^m \lambda_B^n \lambda_C^p \, \mathrm{d}(x, y) = \frac{m!n!p!}{(m + n + p + 2)!} \, 2\,|T|, \quad m, n, p = 0, 1, 2, \ldots,$$

mentioned in [7, p. 201] and proved in [16].

The well known identity (17) or its equivalent variants can be found at many places, see for example [2, 9, 31] etc. Finally, (16) follows from (17) because

$$|\nabla\lambda_A|^2 + \nabla\lambda_A \cdot \nabla\lambda_B + \nabla\lambda_A \cdot \nabla\lambda_C = 0.$$

■

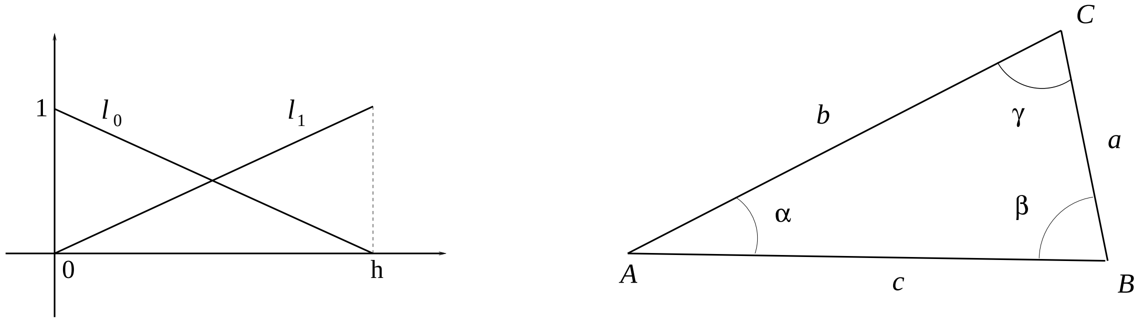

Figure 1: Basic denotation for 1D and 2D linear finite elements.

Lemma 3 *Let $I = (0, d)$ be an interval, T be a triangle, and let $P = T \times I$ be a prism. Adopt the notation from Figure 2, in particular denote by A, B, D, and E the four vertices of an arbitrary rectangular face of the prism P. Further, let $\lambda_A(x, y)$ and $\lambda_B(x, y)$ be the barycentric coordinates corresponding to the vertices A and B of the triangle T and let $\ell_0(z) = 1 - z/d$ and $\ell_1(z) = z/d$. If*

$$\varphi_A(x,y,z) = \lambda_A(x,y)\ell_0(z), \quad \varphi_B(x,y,z) = \lambda_B(x,y)\ell_0(z),$$
$$\varphi_D(x,y,z) = \lambda_A(x,y)\ell_1(z), \quad \varphi_E(x,y,z) = \lambda_B(x,y)\ell_1(z),$$

then

$$\int_P \nabla\varphi_A \cdot \nabla\varphi_B \,\mathrm{d}(x,y,z) = -\frac{d}{12}\left(2\cot\gamma - \frac{|T|}{d^2}\right), \tag{18}$$
$$\int_P \nabla\varphi_A \cdot \nabla\varphi_D \,\mathrm{d}(x,y,z) = \frac{d}{12}\left(\cot\beta + \cot\gamma - \frac{2|T|}{d^2}\right), \tag{19}$$
$$\int_P \nabla\varphi_A \cdot \nabla\varphi_E \,\mathrm{d}(x,y,z) = -\frac{d}{12}\left(\cot\gamma + \frac{|T|}{d^2}\right), \tag{20}$$

and

$$\int_P \varphi_A\varphi_B \,\mathrm{d}(x,y,z) = \frac{d\,|T|}{36}, \tag{21}$$
$$\int_P \varphi_A\varphi_D \,\mathrm{d}(x,y,z) = \frac{d\,|T|}{36}, \tag{22}$$
$$\int_P \varphi_A\varphi_E \,\mathrm{d}(x,y,z) = \frac{d\,|T|}{72}. \tag{23}$$

P r o o f : The statements (21)–(23) simply follow from the results of Lemmas 1 and 2. The integrals (18)–(20) are computed as follows

$$
\begin{aligned}
\int_P \nabla\varphi_A \cdot \nabla\varphi_B \,\mathrm{d}(x,y,z) &= \int_T \nabla\lambda_A \cdot \nabla\lambda_B \,\mathrm{d}(x,y) \int_I \ell_0^2 \,\mathrm{d}z + \int_T \lambda_A\lambda_B \,\mathrm{d}(x,y) \int_I (\ell_0')^2 \,\mathrm{d}z \\
&= -\frac{1}{2}\cot\gamma\,\frac{d}{3} + \frac{|T|}{12}\,\frac{1}{d}, \\
\int_P \nabla\varphi_A \cdot \nabla\varphi_D \,\mathrm{d}(x,y,z) &= \int_T |\nabla\lambda_A|^2 \,\mathrm{d}(x,y) \int_I \ell_0\ell_1 \,\mathrm{d}z + \int_T \lambda_A^2 \,\mathrm{d}(x,y) \int_I \ell_0'\ell_1' \,\mathrm{d}z \\
&= \frac{1}{2}(\cot\beta + \cot\gamma)\,\frac{d}{6} - \frac{|T|}{6}\,\frac{1}{d}, \\
\int_P \nabla\varphi_A \cdot \nabla\varphi_E \,\mathrm{d}(x,y,z) &= \int_T \nabla\lambda_A \cdot \nabla\lambda_B \,\mathrm{d}(x,y) \int_I \ell_0\ell_1 \,\mathrm{d}z + \int_T \lambda_A\lambda_B \,\mathrm{d}(x,y) \int_I \ell_0'\ell_1' \,\mathrm{d}z \\
&= -\frac{1}{2}\cot\gamma\,\frac{d}{6} - \frac{|T|}{12}\,\frac{1}{d}.
\end{aligned}
$$

■

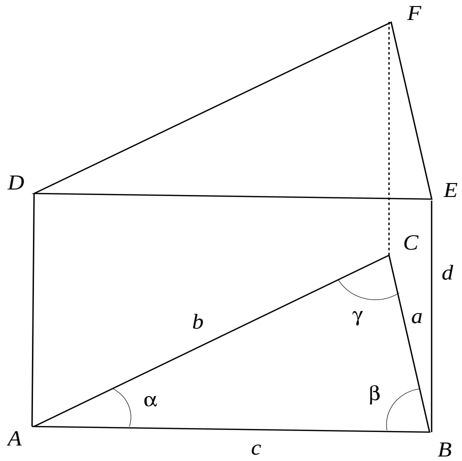

Figure 2: Basic denotation for the prismatic element.

In what follows, all inequalities between matrices, vectors, and scalars are to be understood entrywise. For example, the symbol $\mathbf{A} \geq 0$ means that all entries of a matrix $\mathbf{A} = (a_{ij})_{i,j=1}^N$ are nonnegative, i.e., $a_{ij} \geq 0$ for all $i, j = 1, 2, \ldots, N$.

Definition 3 *Let $P = T \times I$ be a prism and let $\alpha_{\max}^{(T)} \geq \alpha_{\text{mid}}^{(T)} \geq \alpha_{\min}^{(T)} > 0$ be the maximal, medium, and minimal angle of the triangular base T of the prism P, respectively. We define the lower and upper bounds for the altitude of the prism P as*

$$
d_L^{(P)} = \left(\frac{2\cot\alpha_{\max}^{(T)}}{|T|} - \frac{\|c\|_{\infty,P}}{3} \right)^{-1/2} \quad \textit{and} \quad d_U^{(P)} = \left(\frac{\|c\|_{\infty,P}}{6} + \frac{\cot\alpha_{\text{mid}}^{(T)} + \cot\alpha_{\min}^{(T)}}{2\,|T|} \right)^{-1/2}. \tag{24}
$$

The lower bound $d_L^{(P)}$ is well defined only if $\dfrac{2\cot\alpha_{\max}^{(T)}}{|T|} - \dfrac{\|c\|_{\infty,P}}{3} > 0.$

Notice that $\alpha_{\text{mid}}^{(T)} < \pi/2$ and $\alpha_{\text{mid}}^{(T)} < \pi/2$ for any triangle. Thus, $d_U^{(P)}$ is always well defined by (24).

Theorem 2 *Let $\mathcal{T}_{h,\tau}$ be a prismatic partition of Ω. For a prism $P \in \mathcal{T}_{h,\tau}$, let $d_L^{(P)}$ and $d_U^{(P)}$ be defined by (24), and let $d^{(P)}$ denote the altitude of the prism P. If*

$$d_L^{(P)} \leq d^{(P)} \leq d_U^{(P)} \quad \textit{for all } P \in \mathcal{T}_{h,\tau}, \tag{25}$$

then problem (5) *satisfies the DMP according to Definition 1.*

P r o o f : We have

$$a_{ij} = \sum_{P \subseteq \operatorname{supp} \phi_i \cap \operatorname{supp} \phi_j} \int_P \Big(\nabla \phi_i \cdot \nabla \phi_j + c\, \phi_i \phi_j \Big)\, d(x,y,z) = \sum_{P \subseteq \operatorname{supp} \phi_i \cap \operatorname{supp} \phi_j} a_{ij}^{(P)}.$$

As the finite element matrix is symmetric and positive definite, we only need to show that

$$a_{ij}^{(P)} \leq 0 \tag{26}$$

for all $i \neq j$. Then the matrix $\mathbf{A}$ is a Stieltjes matrix, hence, $\mathbf{A}^{-1} \geq 0$. Further, because $\phi_i \geq 0$ for all $i = 1, \ldots, N$, and $f \leq 0$, we have $F_i \leq 0$. Thus, by (9), we obtain $\mathbf{y} \leq 0$ and the DMP (7) holds.

It remains to prove (26). Let us consider a prism $P \in \mathcal{T}_{h,\tau}$, $P = T \times I$, and adopt the notation from Lemma 3, see Figure 2. In particular, we use the short-hand notation $d = d^{(P)}$ for the altitude of the prism. Since we assume that $d_L^{(P)}$ is well defined, we can reformulate conditions (24)–(25) equivalently as

$$-2 \cot \alpha_{\mathrm{max}}^{(T)} + \frac{|T|}{d^2} + \|c\|_{\infty,P} \frac{|T|}{3} \leq 0 \tag{27}$$

and

$$\|c\|_{\infty,P} \frac{|T|}{3} - \frac{2|T|}{d^2} + \cot \alpha_{\mathrm{mid}}^{(T)} + \cot \alpha_{\mathrm{min}}^{(T)} \leq 0. \tag{28}$$

To compute all the entries $a_{ij}^{(P)}$ of the local finite element matrix it is enough to distinguish the following three different cases, see Figure 3.

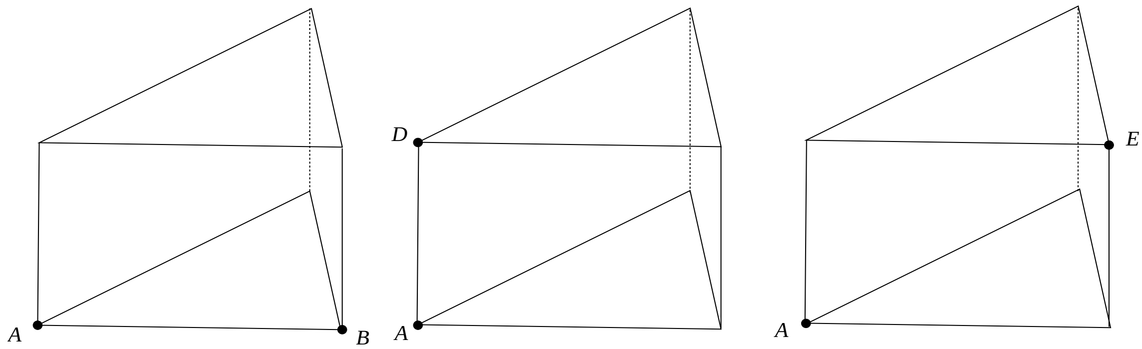

Figure 3: Illustration of node positions in cases (i), (ii), and (iii).

(i) Let A be any vertex of P and let B be one of the two remaining vertices in the same triangular base. If the basis functions ϕ_i and ϕ_j correspond to the vertices A and B, respectively, then by (18) and (21)

$$a_{ij}^{(P)} = \int_P \nabla \varphi_A \cdot \nabla \varphi_B + \int_P c\, \varphi_A \varphi_B \leq \frac{d}{12} \left(-2 \cot \gamma + \frac{|T|}{d^2} + \|c\|_{\infty,P} \frac{|T|}{3} \right). \tag{29}$$

The nonpositivity of this value is guaranteed by (27) because the cotangent is a decreasing function and hence $-\cot\gamma \le -\cot\alpha_{\max}^{(T)}$.

(ii) Let A be any vertex of P and let D be the vertex in the opposite triangular base joined with A by an edge. If the basis functions ϕ_i and ϕ_j correspond to the vertices A and D, respectively, then by (19) and (22)

$$a_{ij}^{(P)} = \int_P \nabla\varphi_A \cdot \nabla\varphi_D + \int_P c\,\varphi_A\varphi_D \le \frac{d}{12}\left(\cot\beta + \cot\gamma - \frac{2|T|}{d^2} + \|c\|_{\infty,P}\,\frac{|T|}{3}\right). \quad (30)$$

The nonpositivity of this value follows from (28) because $\cot\beta + \cot\gamma \le \cot\alpha_{\mathrm{mid}}^{(T)} + \cot\alpha_{\min}^{(T)}$.

(iii) Let A be any vertex of P and let E be the vertex in the opposite triangular base not joined with A by any edge. If the basis functions ϕ_i and ϕ_j correspond to the vertices A and E, respectively, then by (20) and (23)

$$\begin{aligned} a_{ij}^{(P)} = \int_P \nabla\varphi_A \cdot \nabla\varphi_E + \int_P c\,\varphi_A\varphi_E &\le -\frac{d}{12}\left(\cot\gamma + \frac{|T|}{d^2} - \|c\|_{\infty,P}\,\frac{|T|}{6}\right) \\ &= \frac{d}{24}\left(-2\cot\gamma + \frac{|T|}{d^2} + \|c\|_{\infty,P}\,\frac{|T|}{3}\right) - \frac{3d}{24}\frac{|T|}{d^2}. \quad (31) \end{aligned}$$

This is, clearly, nonpositive due to case (i), see (29). ■

5 Construction of meshes for the DMP

It is not immediately clear, how the prismatic partitions satisfying the crucial conditions (24)–(25) look like. In this section, we prove several results which characterize prismatic partitions with property (24)–(25). First of all, we present Lemma 4 which states that conditions (24)–(25) are sharp in the sense that their violation leads to positive entries in the local finite element matrices in certain situations.

Lemma 4 *Let $\mathcal{T}_{h,\tau}$ be a prismatic partition of Ω and let the reaction coefficient c be piecewise constant so that $c|_P = \mathrm{const.}$ for all prisms P in $\mathcal{T}_{h,\tau}$. Then all the off-diagonal entries of the local finite element matrices $a_{ij}^{(P)}$ are nonnegative if and only if conditions (24)–(25) are satisfied.*

P r o o f : The "if" part is a special case of Theorem 2. The "only if" part follows from the fact that (29), (30), and (31) hold in our case as equalities because $\|c\|_{\infty,P} = c|_P$. Thus, if (24)–(25) is not valid then at least one of entries (29) or (30) is positive. ■

In the following proofs we implicitly assume that $d_L^{(P)}$ is well defined and we use an equivalent reformulation of conditions (24)–(25)

$$\frac{\|c\|_{\infty,P}}{6}|T| + \frac{\cot\alpha_{\mathrm{mid}}^{(T)} + \cot\alpha_{\min}^{(T)}}{2} \le \frac{|T|}{(d^{(P)})^2} \le 2\cot\alpha_{\max}^{(T)} - \frac{\|c\|_{\infty,P}}{3}|T|. \quad (32)$$

Below, Lemma 5 shows important observation about the uniform (global) refinement of the prismatic partitions satisfying (24)–(25).

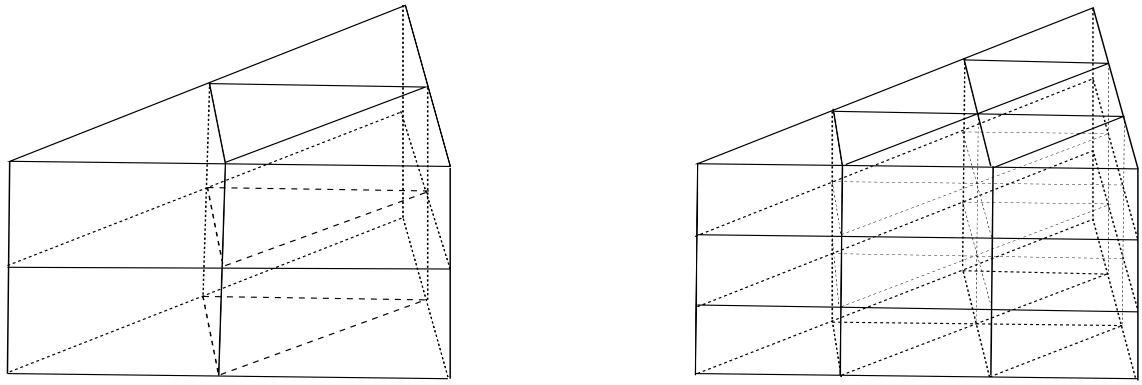

Figure 4: 2-fold and 3-fold uniform refinement of a prism.

Definition 4 *Let m be a positive integer and $\mathcal{T}_{h,\tau}$ be a prismatic partition of Ω. We refine each edge in $\mathcal{T}_{h,\tau}$ into m subedges. Hence, for each prism $P \in \mathcal{T}_{h,\tau}$, $P = T \times I$, we refine the triangular base T into m^2 similar triangles $\widetilde{T}_i \subset T$, $i = 1, 2, \ldots, m^2$, each segment I into m equal segments $\tilde{I}_j \subset I$, $j = 1, 2, \ldots, m$, and we obtain m^3 prisms $\widetilde{P}_{i,j} = \widetilde{T}_i \times \tilde{I}_j$, $\widetilde{P}_{i,j} \subset P$. These prisms $\widetilde{P}_{i,j}$ form a new face-to-face prismatic partition $\widetilde{\mathcal{T}}_{h,\tau}$ of Ω which we call m-fold uniform refinement of $\mathcal{T}_{h,\tau}$. If $m = 1$ then $\widetilde{\mathcal{T}}_{h,\tau} = \mathcal{T}_{h,\tau}$. See Figure 4 for an illustration.*

Lemma 5 *If a prismatic partion $\mathcal{T}_{h,\tau}$ satisfies (24)–(25) then its m-fold uniform refinement $\widetilde{\mathcal{T}}_{h,\tau}$ with $m \geq 1$ satisfies (24)–(25) as well.*

P r o o f : Let $P \in \mathcal{T}_{h,\tau}$, $P = T \times I$, and $\widetilde{P} \in \widetilde{\mathcal{T}}_{h,\tau}$, $\widetilde{P} = \widetilde{T} \times \widetilde{I}$, be such that $\widetilde{P} \subset P$. Then $m^2|\widetilde{T}| = |T|$ and $m\tilde{d} = d$, where d and $\tilde{d}$ stand for the altitudes of prisms P and $\widetilde{P}$, respectively. In addition, the triangles T and $\widetilde{T}$ are similar and therefore the corresponding maximal, medium, and minimal angles $\alpha \geq \beta \geq \gamma$ in T and $\tilde{\alpha} \geq \tilde{\beta} \geq \tilde{\gamma}$ in $\widetilde{T}$ are equal.

Since conditions (24)–(25) and, equivalently, (32) are valid for P, we estimate

$$\frac{\|c\|_{\infty,\widetilde{P}}}{6}|\widetilde{T}| + \frac{\cot\tilde{\beta} + \cot\tilde{\gamma}}{2} \leq \frac{\|c\|_{\infty,P}}{6}\frac{|T|}{m^2} + \frac{\cot\beta + \cot\gamma}{2}$$
$$\leq \frac{|T|}{d^2} \leq 2\cot\alpha - \frac{\|c\|_{\infty,P}}{3}\frac{|T|}{m^2} \leq 2\cot\tilde{\alpha} - \frac{\|c\|_{\infty,\widetilde{P}}}{3}|\widetilde{T}|, \quad (33)$$

where we use the facts that $\|c\|_{\infty,\widetilde{P}} \leq \|c\|_{\infty,P}$ and $m \geq 1$. To finish the proof we realize that inequalities (33) actually prove conditions (32) for the prism $\widetilde{P}$ because $|T|/d^2 = |\widetilde{T}|/\tilde{d}^2$. ■

The following definition and the subsequent theorems provide easily verifyable sufficient conditions for prismatic partitions that yield the DMP. Furthermore, they give practical hints how to construct such partitions.

Definition 5 *Let $\mathcal{T}_{h,\tau} = \mathcal{T}_h^{\mathcal{G}} \times \mathcal{T}_\tau^{\mathcal{I}}$ be a prismatic partion of a cylindrical domain $\Omega = \mathcal{G} \times \mathcal{I} \subset \mathbf{R}^3$, where $\mathcal{G} \subset \mathbf{R}^2$ is a polygon and $\mathcal{I} \subset \mathbf{R}$ is an interval. Further we denote by d_i, $i = 1, 2, \ldots, M$, the lengths of the M segments in $\mathcal{T}_\tau^{\mathcal{I}}$, by $T_{\max}$ and $T_{\min}$ the triangles in $\mathcal{T}_h^{\mathcal{G}}$ with the largest and smallest areas, respectively, and by $\alpha_{\max}^{\mathcal{T}_h^{\mathcal{G}}}$ and $\alpha_{\min}^{\mathcal{T}_h^{\mathcal{G}}}$ the maximal and minimal angles in the triangulation $\mathcal{T}_h^{\mathcal{G}}$, respectively.*

We say that the prismatic partition $\mathcal{T}_{h,\tau}$ is well-shaped *for the DMP if* $\alpha_{\max}^{\mathcal{T}_h^{\mathcal{G}}} < \pi/2$ *and if*

$$\frac{1}{2}|T_{\max}|\tan\alpha_{\max}^{\mathcal{T}_h^{\mathcal{G}}} \le d_i^2 \le |T_{\min}|\tan\alpha_{\min}^{\mathcal{T}_h^{\mathcal{G}}} \quad \forall i = 1,2,\ldots,M. \tag{34}$$

In addition, if $\alpha_{\max}^{\mathcal{T}_h^{\mathcal{G}}} < \pi/2$ *and if*

$$\frac{1}{2}|T_{\max}|\tan\alpha_{\max}^{\mathcal{T}_h^{\mathcal{G}}} < d_i^2 < |T_{\min}|\tan\alpha_{\min}^{\mathcal{T}_h^{\mathcal{G}}} \quad \forall i = 1,2,\ldots,M, \tag{35}$$

then the prismatic partition $\mathcal{T}_{h,\tau}$ is called strictly well-shaped *for the DMP.*

Clearly, a strictly well-shaped partition is also well-shaped. Furthermore, it is easy to see that any m-fold uniform refinement of a (strictly) well-shaped prismatic partition is again (strictly) well-shaped. Hence, we can say that conditions (34) and (35) limit the shape of the prisms and not their actual size. Before we introduce theorems stating that well-shaped partitions guarantee the DMP we present Lemma 6 which presents geometric properties of the well-shaped prismatic partitions. In particular, it limits the maximal angle much more than the technical assumption $\alpha_{\max}^{\mathcal{T}_h^{\mathcal{G}}} < \pi/2$.

Lemma 6 *Let $\mathcal{T}_{h,\tau} = \mathcal{T}_h^{\mathcal{G}} \times \mathcal{T}_\tau^{\mathcal{I}}$ be a well-shaped prismatic partition of a cylindrical domain $\Omega = \mathcal{G} \times \mathcal{I}$. Let $T_{\max}$, $T_{\min}$, $\alpha_{\max}^{\mathcal{T}_h^{\mathcal{G}}}$, and $\alpha_{\min}^{\mathcal{T}_h^{\mathcal{G}}}$ have the same meaning as in Definition 5. Then*

$$\alpha_{\max}^{\mathcal{T}_h^{\mathcal{G}}} \le \arctan\sqrt{8} \approx 70.5288^\circ, \tag{36}$$

$$\alpha_{\min}^{\mathcal{T}_h^{\mathcal{G}}} \ge \arctan(\sqrt{5}/2) \approx 48.1897^\circ, \tag{37}$$

and

$$\frac{|T_{\max}|}{|T_{\min}|} \le 2. \tag{38}$$

P r o o f : We prove this lemma by contradiction. If a prismatic partition $\mathcal{T}_{h,\tau} = \mathcal{T}_h^{\mathcal{G}} \times \mathcal{T}_\tau^{\mathcal{I}}$ is well-shaped for the DMP then

$$\frac{1}{2}|T_{\max}|\tan\alpha_{\max}^{\mathcal{T}_h^{\mathcal{G}}} \le |T_{\min}|\tan\alpha_{\min}^{\mathcal{T}_h^{\mathcal{G}}} \tag{39}$$

independently from the partition $\mathcal{T}_\tau^{\mathcal{I}}$ of $\mathcal{I}$.

Let us suppose that (36) is not valid and let us consider the triangle $T \in \mathcal{T}_h^{\mathcal{G}}$ such that its greatest angle $\alpha = \alpha_{\max}^{\mathcal{T}_h^{\mathcal{G}}} > \arctan\sqrt{8} = 2\arctan(\sqrt{2}/2)$. The smallest angle γ in this T satisfies $\gamma \le \pi/2 - \alpha/2$ which is equivalent to $\cot\gamma \ge \cot(\pi/2 - \alpha/2)$. It can easily be verified that the inequality $\alpha > 2\arctan(\sqrt{2}/2)$ is equivalent to the inequality $2\cot\alpha < \cot(\pi/2 - \alpha/2)$. Thus, $2\cot\alpha < \cot\gamma$. From (39) and from the technical assumption $\alpha_{\max}^{\mathcal{T}_h^{\mathcal{G}}} < \pi/2$ we conclude that

$$1 \le \frac{|T_{\max}|}{|T_{\min}|} \le \frac{2\cot\alpha_{\max}^{\mathcal{T}_h^{\mathcal{G}}}}{\cot\alpha_{\min}^{\mathcal{T}_h^{\mathcal{G}}}} \le \frac{2\cot\alpha}{\cot\gamma} < 1, \tag{40}$$

which is a contradiction and (36) is proved.

To prove (37) by contradition, we consider the triangle $T \in \mathcal{T}_h^{\mathcal{G}}$ such that its smallest angle $\gamma = \alpha_{\min}^{\mathcal{T}_h^{\mathcal{G}}} < \arctan(\sqrt{5}/2) = 2\arctan(1/\sqrt{5})$. The greatest angle α in this T satisfies $\alpha \geq \pi/2 - \gamma/2$ which is equivalent to $\cot\alpha \leq \cot(\pi/2-\gamma/2)$. It can easily be verified that the inequality $\gamma < 2\arctan(1/\sqrt{5})$ is equivalent to the inequality $2\cot(\pi/2-\gamma/2) < \cot\gamma$. Thus, $2\cot\alpha < \cot\gamma$ which is a contradiction due to (40).

Finally, if (38) was not true then (39) together with the inequality $\tan\alpha_{\min}^{\mathcal{T}_h^{\mathcal{G}}} \leq \tan\alpha_{\max}^{\mathcal{T}_h^{\mathcal{G}}}$ would imply

$$2 < \frac{|T_{\max}|}{|T_{\min}|} \leq \frac{2\tan\alpha_{\min}^{\mathcal{T}_h^{\mathcal{G}}}}{\tan\alpha_{\max}^{\mathcal{T}_h^{\mathcal{G}}}} \leq 2, \tag{41}$$

which is a contradiction, again. ■

Notice that the strictly well-shaped prismatic partitions satisfy (36)–(38) with strict inequalities.

We would like to emphasize that conditions (36) and (37) are sharp in the sense that there exist well-shaped prismatic partitions with the maximal and minimal angle equal to $\arctan\sqrt{8}$ and $\arctan(\sqrt{5}/2)$, respectively. Let us construct two examples of such well-shaped prismatic partitions.

(i) Let $\mathcal{T}_{h,\tau}^{(\mathrm{i})}$ consists of copies of a prism $P = T \times I$ whose base T is an isosceles triangle with angles $\alpha = \arctan\sqrt{8} \approx 70.5288°$ and $\beta = \gamma = \pi/2 - \alpha/2 \approx 54.7356°$. If the altitudes of all these prisms are set by (24) to be $d^2 = \left(d_L^{(P)}\right)^2 = \left(d_U^{(P)}\right)^2 = \sqrt{2}|T|$, then this prismatic partition $\mathcal{T}_{h,\tau}$ is well-shaped for the DMP. See Figure 5(i).

(ii) Similarly, to show that (37) is sharp, we construct a prismatic partition $\mathcal{T}_{h,\tau}^{(\mathrm{ii})}$ consisting of prisms with bases T being isosceles triangles with angles $\gamma = \arctan(\sqrt{5}/2) \approx 48.1897°$ and $\alpha = \beta = \pi/2 - \gamma/2 \approx 65.905°$. If the altitudes of these prisms are chosen in agreement with (24) inbetween

$$\frac{1}{2}\sqrt{5}|T| = \left(d_L^{(P)}\right)^2 \leq d^2 \leq \left(d_U^{(P)}\right)^2 = \frac{2}{3}\sqrt{5}|T|$$

then this prismatic partition is well-shaped for the DMP. See Figure 5(ii) for an illustration. Notice that the whole plane $\mathbf{R}^2$ can be tiled by copies of any isosceles triangle.

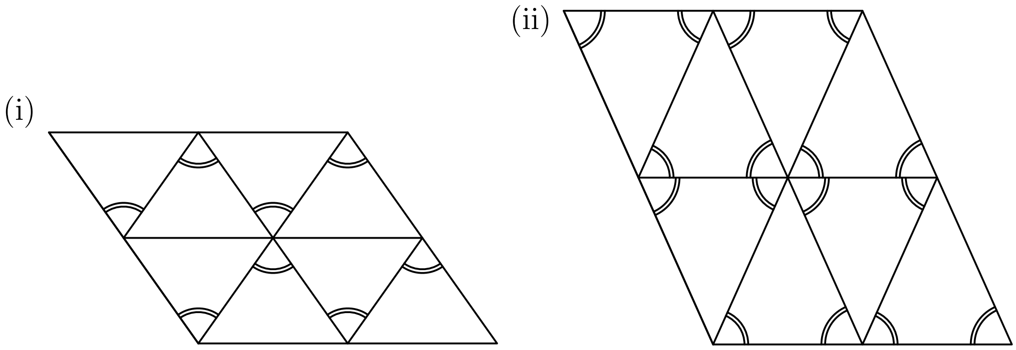

Figure 5: Two examples of isosceles triangulations. (i) The greater angles (70.5288°) are marked by double arcs and the smaller angles (54.7356°) have no mark. (ii) The greater angles (65.905°) are marked by double arcs and the smaller angles (48.19°) have no mark.

On the other hand, condition (38) is not sharp in this sense. A well-shaped prismatic partition such that $|T_{\max}|/|T_{\min}| = 2$ does not exists. Indeed, if $|T_{\max}|/|T_{\min}| = 2$ then (41) implies that $\alpha_{\min}^{\mathcal{T}_h^{\mathcal{G}}} = \alpha_{\max}^{\mathcal{T}_h^{\mathcal{G}}}$, hence all triangles in the triangulation $\mathcal{T}_h^{\mathcal{G}}$ are equilateral and consequently all of them have equal areas. This contradicts the fact that $|T_{\max}|/|T_{\min}| = 2$. Nevertheless, for any $\varepsilon > 0$, it is possible to construct a well-shaped prismatic partition such that $|T_{\max}|/|T_{\min}| = 2 - \varepsilon$. Figure 6 illustrates the construction of the base triangulation for such prismatic partitions. For example, to have $1.99 < |T_{\max}|/|T_{\min}| < 2$ it is enough to set $\omega = 0.03°$ and construct 381 ($n = 380$) triangles according to Figure 6. If the altitudes of the prisms satisfy $0.749029 < d^2 < 0.749546$ then the resulting prismatic partition is strictly well-shaped. There are no interior points in Figure 6. In order to obtain some we can uniformly refine the indicated partition or we can mirror the triangulation with respect to the (almost) horizontal lines.

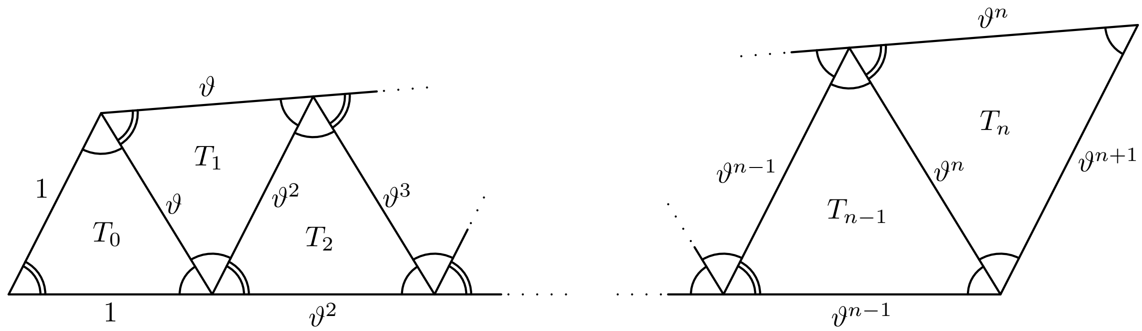

Figure 6: Construction of a triangulation consiting of isosceles triangles which are close to equilateral triangles and whose areas grow such that $|T_n|/|T_0|$ is close to 2. The angles marked by double arcs are equal to $\pi/3 + 2\omega$ and the ones marked by single arcs are $\pi/3 - \omega$, where ω is a small positive angle. If a stands for the lengths of two sides of the isosceles triangle with angle $\pi/3 + 2\omega$ inbetween them then the third side has length ϑa, where $\vartheta = 2\sin(\pi/3 + \omega)$.

The practical significance of Lemma 6 lies in the fact that it gives necessary conditions for a partition to be well-shaped for the DMP. If at least one condition of (36)–(38) is not satisfied then the corresponding prismatic partition is not well-shaped for the DMP. The following theorem says that well-shaped prismatic partitions yield the DMP in the pure diffusion case, i.e., for $c \equiv 0$ in Ω.

Theorem 3 *Let $\Omega = \mathcal{G} \times \mathcal{I} \subset \mathbf{R}^3$ be a cylindrical domain and let $\mathcal{T}_{h,\tau} = \mathcal{T}_h^{\mathcal{G}} \times \mathcal{T}_\tau^{\mathcal{I}}$ be its well-shaped prismatic partition. If $c \equiv 0$ in Ω, then discretization* (5) *based on the prismatic partition $\mathcal{T}_{h,\tau}$ satisfies the DMP according to Definition 1.*

P r o o f : Lemma 6, statement (36), implies that all angles in the triangulation $\mathcal{T}_h^{\mathcal{G}}$ are well below $\pi/2$. Hence, tangents and cotangents of all angles in $\mathcal{T}_h^{\mathcal{G}}$ are positive.

Let us consider a prism $P = T \times I$ in $\mathcal{T}_{h,\tau}$. Further, let $\alpha \geq \beta \geq \gamma > 0$ be the angles in the triangle T, and let d stand for the altitude of the prism P. The assumption (34) implies

$$\frac{\cot\beta + \cot\gamma}{2} \leq \frac{|T|}{|T_{\min}|} \cot \alpha_{\min}^{\mathcal{T}_h^{\mathcal{G}}} \leq \frac{|T|}{d^2} \leq \frac{|T|}{|T_{\max}|} 2 \cot \alpha_{\max}^{\mathcal{T}_h^{\mathcal{G}}} \leq 2\cot\alpha.$$

Thus, conditions (32) and, equivalently, (24)–(25) are satisfied for all prisms $P \in \mathcal{T}_{h,\tau}$ and Theorem 2 concludes the proof. ■

Theorem 4 below characterizes a class of prismatic partitions which provide the DMP in the general diffusion-reaction case $c \geq 0$ in Ω. Such partitions must be *strictly* well-shaped and fine enough. Moreover, Theorem 4 quantifies how fine the suitable partitions must be.

Theorem 4 *Let $\Omega = \mathcal{G} \times \mathcal{I} \subset \mathbf{R}^3$ be a cylindrical domain and let $\mathcal{T}_{h,\tau} = \mathcal{T}_h^{\mathcal{G}} \times \mathcal{T}_\tau^{\mathcal{I}}$ be its strictly well-shaped prismatic partition. Furthermore, let $m \geq 1$ be an integer such that*

$$m^2 \geq \max_{P \in \mathcal{T}_{h,\tau}} \frac{\|c\|_{\infty,P} |T|}{M_P}, \tag{42}$$

where $P = T \times I$ is a prism and

$$M_P = \min \left\{ 6 \left(\frac{|T|}{d^2} - \frac{\cot\beta + \cot\gamma}{2} \right),\ 3 \left(2\cot\alpha - \frac{|T|}{d^2} \right) \right\}, \tag{43}$$

with $\alpha \geq \beta \geq \gamma$ being the angles in the triangle T and d standing for the altitude of the prism P. Then discretization (5) based on the m-fold uniform refinement $\widetilde{\mathcal{T}}_{h,\tau}$ of $\mathcal{T}_{h,\tau}$ satisfies the DMP according to Definition 1.

P r o o f : Let us consider the m-fold uniform refinement $\widetilde{\mathcal{T}}_{h,\tau}$ of the strictly well-shaped prismatic partition $\mathcal{T}_{h,\tau}$ with $m \geq 1$ given by (42). Let $\widetilde{P} = \widetilde{T} \times \tilde{I}$ be a prism in $\widetilde{\mathcal{T}}_{h,\tau}$ and let $P \in \mathcal{T}_{h,\tau}$, $P = T \times I$, be such a prism that $\widetilde{P} \subset P$. Denote by $\tilde{d}$ and d the altitudes of prisms $\widetilde{P}$ and P, respectively. Clearly, $m^2|\widetilde{T}| = |T|$, $m\tilde{d} = d$, and the triangles $\widetilde{T}$ and T are similar, hence the corresponding angles $\tilde{\alpha} \geq \tilde{\beta} \geq \tilde{\gamma} > 0$ in $\widetilde{T}$ and $\alpha \geq \beta \geq \gamma > 0$ in T are equal. Notice that all angles in both $\mathcal{T}_{h,\tau}$ and $\widetilde{\mathcal{T}}_{h,\tau}$ are acute by Lemma 6.

Since the prismatic partition $\mathcal{T}_{h,\tau}$ is strictly well-shaped we have $M_P > 0$ and assumption (42) implies

$$\|c\|_{\infty,\widetilde{P}} |\widetilde{T}| \leq \|c\|_{\infty,P} \frac{|T|}{m^2} \leq M_P,$$

where we used $\|c\|_{\infty,\widetilde{P}} \leq \|c\|_{\infty,P}$. Hence, from definition (43) we obtain

$$\frac{\|c\|_{\infty,\widetilde{P}} |\widetilde{T}|}{6} + \frac{\cot\tilde{\beta} + \cot\tilde{\gamma}}{2} \leq \frac{|\widetilde{T}|}{\tilde{d}^2} \leq 2\cot\tilde{\alpha} - \frac{\|c\|_{\infty,\widetilde{P}} |\widetilde{T}|}{3},$$

where we utilize the facts that $\tilde{\alpha} = \alpha$, $\tilde{\beta} = \beta$, $\tilde{\gamma} = \gamma$, and $|\widetilde{T}|/\tilde{d}^2 = |T|/d^2$. Thus we verified the validity of conditions (32) and, equivalently, (24)–(25) for all prisms $\widetilde{P} \in \widetilde{\mathcal{T}}_{h,\tau}$ and Theorem 2 finishes the proof. ∎

Remark 2 In the pure diffusion case, i.e., $c \equiv 0$ in Ω, the conditions for validity of the DMP limit the shape and not the size of elements, cf. (32). Indeed, condition (32) limits the ratio of the area of the base triangle and the square of the altitude of the prism by the angles in the base triangle, but the size (volume) of the prism can be made arbitrarily large or small while keeping this ratio constant. On the other hand, in the general case, if the reaction coefficient c does not vanish then the partition must be also fine enough in order to obtain the DMP, cf. Theorem 4. This is typical behavior of the diffusion-reaction problem and it is in agreement with the previous DMP results for problems with the reaction term, see, e.g., [3] for simplicial finite elements.

Remark 3 Conditions (34) and (35) for the well-shaped and the strictly well-shaped prismatic partitions bound the altitudes of the prisms from two sides. Therefore, it could be troublesome or even impossible to divide a given domain $\Omega = \mathcal{G} \times \mathcal{I}$ into layers with suitable altitudes. However, if there exists a triangulation of $\mathcal{G}$ satisfying (39) then for any altitude of Ω exists a sequence of domains $\Omega_k = \mathcal{G} \times \mathcal{I}_k$, such that $\Omega_k \to \Omega$ as $k \to \infty$ and that a (strictly) well-shaped prismatic partition of Ω_k exists. Notice that the domains Ω_k and their (strictly) well-shaped prismatic partitions need not to be necessarily nested.

Remark 4 For illustration let us consider the most favorable triangulation $\mathcal{T}_h^{\mathcal{G}}$ consisting of equilateral triangles with the same area. Let a stands for the length of each side of these triangles. Further, let the reaction coefficient c vanishes. In order to satisfy conditions (24)–(25) and, hence, to obtain the DMP the altitudes d of the prisms in the prismatic partition $\mathcal{T}_{h,\tau} = \mathcal{T}_h^{\mathcal{G}} \times \mathcal{T}_\tau^{\mathcal{I}}$ are limited by

$$\frac{3}{8}a^2 \leq d^2 \leq \frac{3}{4}a^2. \tag{44}$$

6 Numerical tests

In this section, we illustrate the theoretical results by numerical computations. The numerical tests also show that the DMP is valid for much wider class of meshes than the theory predicts.

First, we construct a well shaped triangulation for the DMP according to Definition 5. This triangulation will be used to demonstrate the usage of Lemmas 5 and 6 as well as Theorems 2, 3, and 4. The construction of the well shaped triangulation for the DMP requires some care, however. Lemma 6 gives necessary conditions on the shape of the well shaped triangulations, but sufficient conditions are unclear.

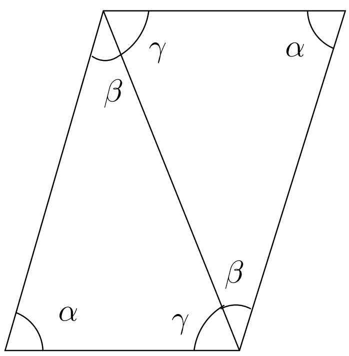

Figure 7: The original partition.

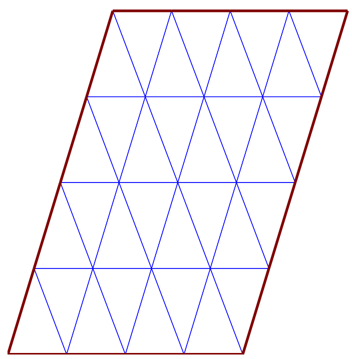

Figure 8: The applied computational mesh.

In order to construct a strictly well shaped prismatic partition we consider a triangulation consisting of similar triangles as presented in Figure 7. All computations are performed using two times refined original partition (4-fold refinement), presented in Figure 8. The prismatic partition is constructed from this triangulation by creating four layers of prismatic elements with equal altitudes d. For this kind of partitions, the well shapedness condition (34) reduces to a simple inequality

$$\frac{1}{2}\tan\alpha_{\max} \leq \tan\alpha_{\min}. \tag{45}$$

We stress that in agreement with (1) we use zero Dirichlet boundary conditions in all computations.

In the first test, we study inequality (45) and its relation to the existence of a suitable altitude d which would yield the DMP for $c = 0$. We compare altitudes predicted by the theory (Theorems 2 and 3) with the altitudes computed numerically. Since the shape of the applied partition (see Figure 7) is determined by the values of $\alpha_{\max}$ and $\alpha_{\min}$, we can visualize the results as a function of these two parameters. This is done in Figure 9. Domain 1 illustrates the set of the well shaped triangulations, according to Definition 5. Triangulations from this set satisfy the DMP by Theorem 3. In our case, domain 1 is determined by (45). Domain 2 is the set of the non well-shaped triangulations, which satisfy the DMP with a suitable altitude d according to Theorem 2. Domain 3 corresponds to the set of triangulations for which we can computationally verify the DMP for a certain altitude d. All other triangulations (domain 4) do not satisfy the DMP for any altitude. We remark that the graining of the image is due to the finite resolution applied in computations. Still, we can verify the sharpness of the necessary bounds for $\alpha_{\min}$ and $\alpha_{\max}$ given by Lemma 6.

In Figure 9, we can compare the set of triangulations, where the DMP is guaranteed by our theoretical results (domains 1 and 2), with the set of all triangulations yielding the DMP (domain 3). We observe that the theory covers considerable part of the triangulations yielding the DMP. On the other hand, this numerical experiment reveals that the set of triangulations yielding the DMP is much wider than the theory predicts.

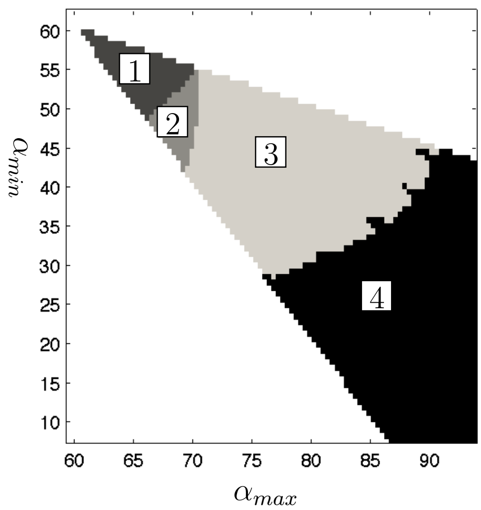

Figure 9: Characterization of the applied partitions according to $\alpha_{\max}$ and $\alpha_{\min}$. In domains 1 and 2, the DMP is guaranteed by Theorem 3 and 2. Domain 3 is not covered by the theory but the DMP is valid there. Partitions corresponding to domain 4 do not yield the DMP at all.

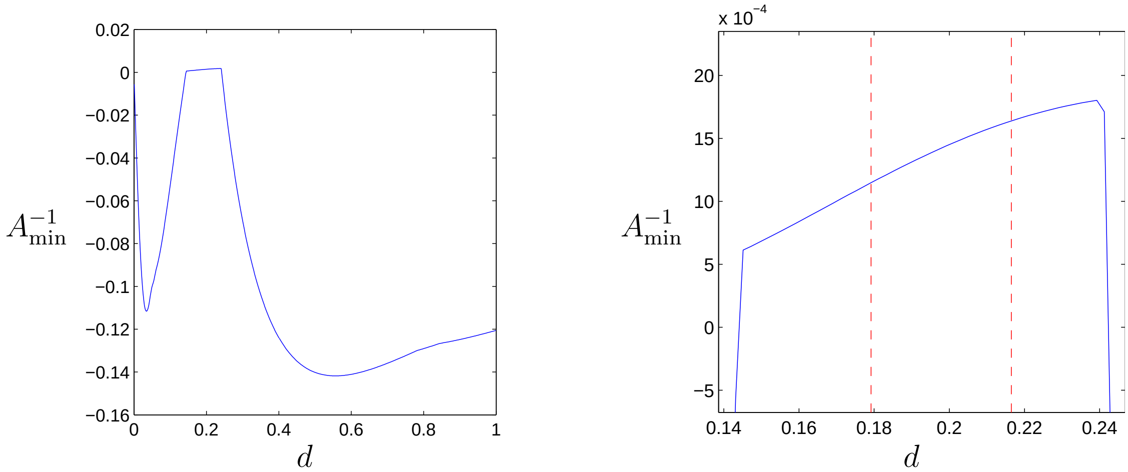

Figure 10: The smallest entry $A^{-1}_{\min} = \min_{ij} A^{-1}_{ij}$ of the inverse of the finite element matrix as a function of the altitude d for $c = 0$ (left). Theoretical bounds (24)–(25) are plotted as the dashed lines (right). The right panel is a zoom from the left panel.

In the second test, we demonstrate the theoretical bounds (24)–(25) for the altitude d in the case $c = 0$, see Theorem 2. For this purpose, we construct a sequence of prismatic partitions. All these partitions are based on the same triangulation and have four layers of prisms with the altitude d varying from 0 to 1 with step 0.002. Based on the first test, we choose as the base triangulation a strictly well-shaped triangulation shown in Figure 8 with angles 65, 60, and 55 degrees. This base triangulation is used also for all the subsequent tests.

For each prismatic partition in the sequence, we find the smallest entry $A^{-1}_{\min}$ of the inverse of the finite element system matrix, $A^{-1}_{\min} = \min_{ij} A^{-1}_{ij}$. As the DMP according to Definition 1 is valid if and only if $A^{-1}_{\min} \geq 0$, this value indicates whether the DMP property is satisfied. The results are visualized in Figure 10. As one can observe, the computationally obtained bounds for the DMP are only little larger compared to the theoretically predicted bounds (24)–(25).

In the third test, we study the behavior of the bounds (24)–(25) for the altitude d, when the coefficient c is a constant greater than zero. We use the same prismatic partitions as in the previous case, but we vary the coefficient c from 1 to 30 with step 1. Theoretically calculated and computationally verified bounds for the altitude d yielding the DMP are visualized as functions of c in Figure 11. In this figure, we observe that the DMP is lost for sufficiently large values of c, as predicted by bounds (24)–(25) presented in Theorem 2. The computational bounds for the DMP behave in a similar manner as the theoretical ones.

Finally, in the fourth test, we study if the DMP can be recovered for $c = 100$ by the m-fold uniform refinement, according to Theorem 4. In this case, the theoretical bounds for the altitude d with $c = 0$ are $d_L = 0.17918$ and $d_U = 0.2165$. The initial altitude was chosen between these bounds as $d_0 = 0.1930$. Figure 12 presents the behavior of the computational and theoretical bounds for d. For the chosen value of the reaction coefficient c, the initial partition does not yield the DMP for any altitude. As the partition is strictly well shaped for the DMP, Theorem 4 states that a three-fold ($M_P = 0.38595$ and $m = 3$) refinement should restore the DMP. This phenomenon is indeed observed in our computations. Nevertheless, the results show an existence of a suitable altitude d

yielding the DMP even for $m = 2$. This test confirms that the DMP is valid for any m-fold uniform refinement with sufficiently large m, as predicted by Lemma 5 and Theorem 4. The theoretically predicted value of m could be, however, greater then it is necessary, in certain situations.

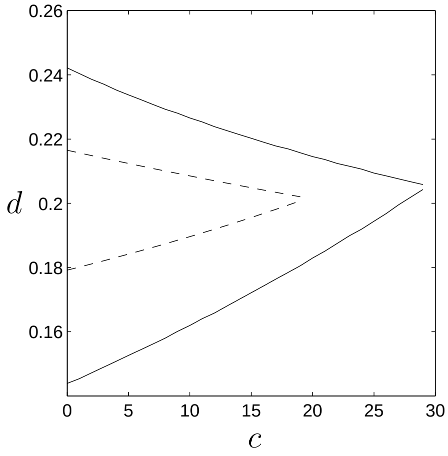

Figure 11: Behavior of the theoretical (dashed lines) and the computational (solid lines) bounds for the altitude d as a function of the coefficient c.

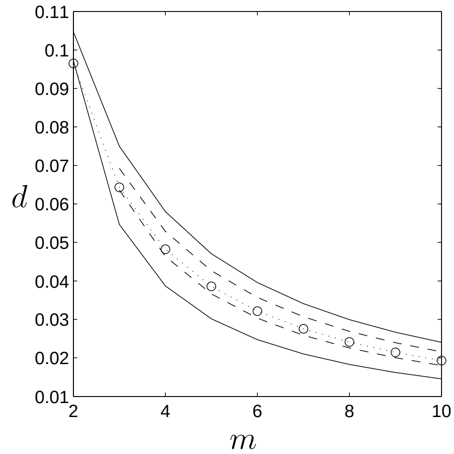

Figure 12: Behavior of the theoretical (dashed lines) and the computational (solid lines) bounds for the altitude d with respect to the m-fold uniform refinement. The dotted line denotes the original altitude $d_0 = 0.1930$ and its refinement. The reaction coefficient is chosen as $c = 100$.

7 Conclusions, generalizations, and open problems

The crucial result of this paper is formulated in Theorem 2, where we present an easily verifyable condition (25) which guarantees the DMP. This theorem, however, does not provide any guidelines how to construct suitable prismatic partitions for the validity of the DMP. Therefore, we developed the concept of the (strictly) well shaped prismatic partitions to characterize the base triangulations which guarantee existence of suitable altitudes of the layers of prisms. The corresponding DMP on the (strictly) well shaped prismatic partitions is formulated and proven in Theorems 3 and 4.

In Section 6, we present various numerical tests to asses the sharpness of the theoretically obtained conditions. The first test, see Figure 9, is of particular interest, because it indicates that the class of partitions which provide the DMP is much wider than one would expect from the theoretical results.

Let us conclude this paper by the following list of possible generalizations and open problems.

- To prove the DMP, we actually require the FE matrix $\mathbf{A}$ to have the nonnegative inverse, i.e., $\mathbf{A}^{-1} \geq 0$. It is well known that some off-diagonal entries can be positive and still one has $\mathbf{A}^{-1} \geq 0$ (see, e.g., a very recent work [1] for a discussion and literature on this subject). This observation was actually used in [20] to weaken the standard condition of nonobtuseness (cf. [4, 19]) for tetrahedral elements. Similar approach can be, obviously, applied to the case of prismatic meshes and conditions (24)–(25) can be thus weakened.

- It would be interesting to investigate the DMPs in the case of the so-called hybrid meshes, consisting of tetrahedra, hexahedra, pyramids, and prisms (see [30]). The goal would be to derive suitable geometric conditions on the shapes of these elements and to propose techniques for refinements (cf. [25]) of such meshes preserving the shape limitations.

- The proofs of the DMPs for parabolic problems usually utilize the geometric conditions derived in the elliptic case, cf. [13] for the simplicial finite elements. The above presented concept of the well-shaped prismatic partitions can be used to prove the DMP for parabolic problems discretized in space variables by prismatic finite elements.

- Similarly, our concept of the well-shaped prismatic partitions can be used to treat the DMPs for nonlinear elliptic problems. It is possible to follow the ideas introduced in [17, 18].

- In recent works [5, 22, 23, 31] the authors try to preserve the DMPs by nonlinear computational schemes which allow to avoid or considerably weaken the geometric limitations on the meshes. These techniques can be generalized to the prismatic finite elements as well.

References

[1] Bouchon, F., Monotonicity of some perturbations of irreducibly diagonally dominant M-matrices, *Numer. Math.* 105 (2007), 591–601.

[2] Brandts, J., Korotov, S., Křížek, M., Dissection of the path-simplex in $\mathbf{R}^n$ into n path-subsimplices, *Linear Algebra Appl.* 421 (2007), 382–393.

[3] Brandts, J., Korotov, S., Křížek, M., The discrete maximum principle for linear simplicial finite element approximations of a reaction-diffusion problem, 16 p., Research report A525, Helsinki University of Technology, 2007, submitted.

[4] Brandts, J., Korotov, S., Křížek, M., Šolc, J., On acute and nonobtuse simplicial partitions, *SIAM Review*, 1–20 (in press).

[5] Burman, E., Ern, A., Discrete maximum principle for Galerkin approximations of the Laplace operator on arbitrary meshes, *C. R. Math. Acad. Sci. Paris* 338 (2004), 641–646.

[6] Ciarlet, P. G., Discrete maximum principle for finite-difference operators, *Aequationes Math.* 4 (1970), 338–352.

[7] Ciarlet, P. G., *The Finite Element Method for Elliptic Problems,* North-Holland, Amsterdam, 1978.

[8] Ciarlet, P. G., Raviart, P.-A., Maximum principle and uniform convergence for the finite element method, *Comput. Methods Appl. Mech. Engrg.* 2 (1973), 17–31.

[9] Drăgănescu, A., Dupont, T., Scott, L. R., Failure of the discrete maximum principle for an elliptic finite element problem, *Math. Comp.* 74 (2005), 1–23.

[10] Faragó, I., Horváth, R., Discrete maximum principle and adequate discretizations of linear parabolic problems, *SIAM J. Sci. Comput.* 28 (2006), 2313–2336.

[11] Faragó, I., Karátson, J., *Numerical Solution of Nonlinear Elliptic Problems via Preconditioning Operators. Theory and Applications.* Advances in Computation, Volume 11, NOVA Science Publishers, New York, 2002.

[12] Fiedler, M., *Special Matrices and Their Applications in Numerical Mathematics* Martinus Nijhoff Publishers, Dordrecht, 1986.

[13] Fujii, H., Some remarks on finite element analysis of time-dependent field problems, *Theory and Practice in Finite element Structural Analysis*, Univ. Tokyo Press, Tokyo (1973), 91–106.

[14] Horváth, R., On the sign-stability of the numerical solutions of the heat equation, *Pure Math. Appl.* 11 (2000), 281–291.

[15] Horváth, R., On the sign-stability of the numerical solutions of one-dimensional parabolic problems, *Appl. Math. Modelling* (in press).

[16] Holand, I., Bell, K., *Finite Element Methods in Stress Analysis,* Tapir, Trondheim, 1969.

[17] Karátson, J., Korotov, S., Discrete maximum principles for finite element solutions of nonlinear elliptic problems with mixed boundary conditions, *Numer. Math.* 99 (2005), 669–698.

[18] Karátson, J., Korotov, S., Křížek, M., On discrete maximum principles for nonlinear elliptic problems, *Math. Comput. Simulation* 76 (2007), 99–108.

[19] Korotov, S., Křížek, M., Acute type refinements of tetrahedral partitions of polyhedral domains, *SIAM J. Numer. Anal.* 39 (2001), 724–733.

[20] Korotov, S., Křížek, M., Neittaanmäki, P., Weakened acute type condition for tetrahedral triangulations and the discrete maximum principle, *Math. Comp.* 70 (2001), 107–119.

[21] Křížek, M., Lin Qun, On diagonal dominance of stiffness matrices in 3D, *East-West J. Numer. Math.* 3 (1995), 59–69.

[22] Kuzmin, D., On the design of algebraic flux correction schemes for quadratic finite elements, *J. Comp. Appl. Math.* (in press).

[23] Lipnikov, K., Shashkov, M., Svyatskiy, D., Vassilevski, Yu., Monotone finite volume schemes for diffusion equations on unstructured triangular and shape-regular polygonal meshes, *J. Comput. Phys.* (to appear).

[24] Protter, M., Weinberger, H., *Maximum principles in differential equations*, Prentice-Hall, Englewood Cliffs, New Jersey, 1967.

[25] Siebert, K. G., Local refinement of 3D-meshes consisting of prisms and conforming closure, *Impact Comput. Sci. Engrg.* 5 (1993), 271–284.

[26] Unterreiter, A., Juengel, A., Discrete minimum and maximum principles for finite element approximations of non-monotone elliptic equations, *Numer. Math.* 99 (2005), 485–508.

[27] Varga, R., *Matrix Iterative Analysis*, Prentice Hall, New Jersey, 1962.

[28] Varga, R., On discrete maximum principle, *J. SIAM Numer. Anal.* 3 (1966), 355–359.

[29] Vejchodský, T., Šolín, P., Discrete maximum principle for higher-order finite elements in 1D, *Math. Comp.* 76 (2007), 1833–1846.

[30] Wieners, C., Conforming discretizations on tetrahedrons, pyramids, prisms and hexahedrons, Univ. Stuttgart, Bericht 97/15, 1–9 (1997).

[31] Xu, J., Zikatanov, L., A monotone finite element scheme for convection-diffusion equations, *Math. Comp.* 68 (1999), 1429–1446.